The role of hydrodynamic and biogeochemistry on CO₂ flux and pCO₂ at the Amazon River mouth

Diani F. S. Less[1,2], Alan C. Cunha[2], Henrique O. Sawakuchi[3,4], Vania Neu[5], Aline M. Valério[6],
Nicholas D. Ward[7,9], Daimio C. Brito[8], Joel E. M. Diniz[2], William Gagne-Maynard[7], Carlos M.
Abreu[2,8], Milton Kampel[6], Alex V. Krusche[3] and Jeffrey E. Richey[9]

[1] Instituto de Ciências e Tecnologia das Águas, Universidade Federal do Oeste do Pará, Santarém, 68040-050, Brasil
[2] Departamento de Meio Ambiente e Desenvolvimento, Universidade Federal do Amapá, Macapá, 68902-280, Brasil
[3] Centro de Energia Nuclear na Agricultura, Universidade de São Paulo, Piracicaba, 13400-970, Brasil
[4] Department of Ecology and Environmental Science, Umeå Universitet. KBC-huset, Linnaeus väg 6, 901 87 Umeå, Sweden
[5] Instituto Sócio Ambiental e dos Recursos Hídricos, Universidade Federal Rural da Amazônia, Belém, 66077-530, Brasil
[6] Divisão de Sensoriamento Remoto, Instituto Nacional de Pesquisas Espaciais, São José dos Campos, 12227-010, Brasil
[7] Marine Sciences Laboratory, Pacific Northwest National Laboratory, Sequim, 98382, USA
[8] Universidade do Estado do Amapá, Macapá, 68.900-070, Brasil
[9] School of Oceanography, University of Washington, Seattle, 98195, USA

Correspondence to: Diani F. S. Less (diani.less@ufopa.edu.br)

Abstract. Recent estimates indicate that the lower Amazon River outgasses significant amounts of carbon dioxide (CO_2) that was not previously accounted for the global inland water carbon budget. Detailed evaluation of seasonal variability and controlling mechanisms behind the CO_2 fluxes in this large and complex area remains incomplete. Previous observations throughout the Amazon basin showed that higher CO_2 fluxes (FCO₂) and partial pressure of CO_2 (pCO₂) occur during high water and higher wind intensity seasons. The influence of wind and water speed, depth of water column, as well as respiration of allochthonous and autochthonous organic matter, are frequently assigned as the main control variables. Here, we assess the influence of a set of biogeochemical and hydrodynamic parameters on the seasonal variation of FCO₂ and pCO₂ near the Amazon River mouth. FCO₂, pCO₂ and biogeochemical and hydrologic analyses were carried out from 2010 to 2016 during four different hydrological periods per year (N=25) in the North Channel of the Amazon River mouth. FCO₂ and pCO₂ were used as dependent variables and analyzed against 33 biogeochemical, hydrodynamic and meteorological parameters along the hydrological seasons. The highest FCO₂ and pCO₂ was obtained at high discharge season (11.28 ± 7.82 µmol m⁻² s⁻¹ and (4575 ± 429 µatm, respectively) when most of these parameters tend to be higher. Among the 33 parameters analyzed, the significant correlations with FCO₂ and pCO₂ ($p<0.05$) observed were for water and air temperatures, dissolved oxygen, dissolved organic carbon, nitrate, dissolved inorganic nitrogen and pH. These variables could be considered suitable predictors for estimating pCO₂ and FCO₂ in the Amazon River mouth area. For a better estimation and understanding of carbon budgets in tropical rivers it is still required to verify and to quantify more deeply the relationship among CO_2 evasion and others hydrodynamic, meteorological and biogeochemical variables.

1 Introduction

Rivers play an active role in the global carbon budget, connecting terrestrial ecosystems to the atmosphere and ocean. The Amazon River is responsible for 20 % (120000 m^3 s^{-1}) of the water discharge to Western Tropical North Atlantic Ocean, being the largest source of freshwater to the ocean (Molinier et al., 1996; Goes et al., 2014).

Inland running waters transported roughly 5.7 Pg C annually. This value represents approximately 75 % of this amount returned to the atmosphere as CO_2 (Le Quéré et al., 2015), with the terrestrial plants being the major source of carbon processed in the river (Richey et al., 2002; Cole et al., 2007; Aufdenkampe et al., 2011).

The most recent estimates shows that Amazon running waters outgasses 1.39 Pg C year^{-1}, increasing the global emissions to 2.9 Pg C year^{-1} from inland waters. This difference represents an increase of about 43 % (Sawakuchi et al., 2017). This value is also approximately an equivalent amount of CO_2 as the rainforest sequesters on an annual basis (Brienen et al., 2015). Therefore, understanding the drivers controlling pCO_2 and CO_2 outgassing is important to improve regional and global scale carbon budget estimates.

Climatic and geomorphological features play an important role on water turbulence and chemistry, which in turn directly affects gas fluxes to the atmosphere. In large rivers, wind speed is one of the major controls on gas transfer velocity (K_{600}) (Borges et al., 2004; Alin et al., 2011; Rasera et al., 2013; Sawakuchi et al., 2017). Likewise, other physical variables such as depth and width of the channel, and the fetch length, vertical mixing and water velocity are also related to the evasive flux (Raymond and Cole, 2001; Rasera et al., 2008; Liu et al., 2017). In streams and small tributaries, seasonality, water velocity and depth are the most important physical parameters, while for mainstem and estuaries wind speed is the main driver related to the gas flow at the air-water interface (Alin et al., 2011).

In the lower Amazon River mainstem, recent studies have shown that the dynamic balance controls the concentration of dissolved CO_2 (Ward et al., 2018), including the inputs from respiration of allochthonous and autochthonous organic matter (Mayorga et al.,, 2005), water-sediments interactions (Devol et al., 1987), floodplains (Melack et al., 2009; Abril et al., 2014), outputs from gas evasion (Richey et al., 2002; Sawakuchi et al., 2017) and *in situ* primary production (Engle et al., 2008; Silva et al., 2009; Gagne-Maynard et al., 2017). Thus, pCO_2 in rivers reflects both, internal carbon dynamics and upstream terrestrial biogeochemical processes that represent the intensity of gas exchange at the water-to-air interface, controlling the source or sink of atmospheric CO_2 for rivers (Richey et al., 2002; Richey, 2003; Elin et al., 2011; Alin et al., 2011; Ward et al, 2013).

However, most studies in the Amazon River basin are concentrated in the central region, which represents ≈ 30% of the total basin area (Hedges et al., 1986; Hedges et al., 2000; Moreira-Turcq et al., 2003). On the other hand, studies in the lower Amazon River are still relatively scarce, with low temporal resolution due to limited logistical access. Besides that, usually, these studies do not consider the influence of a large range of variables (biogeochemical, hydrodynamic and meteorological)

and local factors such as macro and meso tides, strong trade winds and large air-water surface area that promote favorable conditions for CO_2 outgassing (Sawakuchi et al., 2017). The present study aimed to evaluate and identify the most important hydrodynamic, biogeochemical and meteorological factors related to the pCO_2 and FCO_2 at the Amazon River mouth.

2 Methods

2.1 Study area and sampling procedures

The measurements were carried out from 2010 to 2016 in the deepest point of the North Channel in the Amazon River mouth (00°02'872" S 051°04'616" W) near the city of Macapá (Fig. 1) (Table 1 and 2, S1). The North channel represents ~30 % of the Amazon River discharge (Ward et al., 2015). This area is influenced by meso tides that promotes a ~3m variation in river depth amplitude, reversing the river flow with no salinity intrusion (Sawakuchi et al., 2017). In 150 km downstream from Macapá the North Channel remains to widen and channelize between large islands until being completely disconnected from land and the riparian zone/floodplains (Ward et al., 2015; Sawakuchi et al., 2017). Water entering the ocean continues fresh, at the surface, as much as 60 km offshore from this point (Molinas et al., 2014).

Located in the equatorial region, the climate in the study area is characterized by a rainy tropical monsoon climate, type "Am" (Köppen, 1948), warm and humid, with little temperature variation. The annual average air temperature is 26.0 ± 0.4 °C, with maximum and minimum values between 31.5 ± 0.7 °C and 22.0 ± 0.3 °C, respectively (Costa et al., 2013).

The annual average precipitation between 2010-2016 was 2489 ± 209 mm, similar to the historical average (1981-2010) with 2550 mm (INMET, 2017).

Field sampling was carried out based on the hydrographic periods developed by Richey et al., (1990) and following the protocols described in the CAMREX project (Carbon in the Amazon River Experiment), over the last 30 years (Richey et al., 1986, 1990).

Sampling campaigns of 27 biogeochemical, 5 kinetic and 2 thermodynamic variables (Table 1) were done between 2010 and 2016 (N = 25). Surface *in situ* measurements and samples were collected for the biogeochemical analysis. The resulted data set of each field campaign was combined according to four hydrological seasons: rising water season (from Jan to Mar), high water (from Apr to Jun), falling water (from Jul to Sep) and low water (from Oct to Dec) (Valerio et al., 2018). The data analysis was carried out considering the average values of each of the 25 campaigns for the identification of the most influencing parameters on pCO_2 and FCO_2 and for the understanding of their seasonal variability.

2.2 Biogeochemical variables

2.2.1 pCO_2, CO_2 flux and estimation gas transfer velocity (K_{600})

pCO_2 was measured using a headspace equilibration chamber filled with glass beads to increase the exchange surface and reduce the volume of air. The chamber was coupled to an Infrared Gas Analyzer (LICOR Instruments, LI-820) as described

by Frankignoulle et al., (2001). Surface water was collected at approximately 30 cm depth by a submersible pump (Rule 360 Bilge) passing through the chamber from top to bottom at a flow rate of 1.5 L min⁻¹. A diaphragm mini-pump (AS-200; Spectrex) promotes a closed air circuit (150 mL min⁻¹) circulating through the equilibrating chamber through a moisture trap (Drierite) connected to an Infrared Gas Analyzer (Rasera et al., 2008, Sawakuchi et al., 2017).

5   CO_2 fluxes were measured using a floating chamber (volume 10.6 L and 0.1251 m² area) (Rasera et al., 2008). The floating chamber was coupled to a portable Infrared Gas Analyzer using a diaphragm minipump (AS-200; Spectrex) and a desiccating water trap (Drierite). Flux measurements were started after the concentrations were stable with the atmosphere concentration was registered. Chamber measurements were done for approximately 5 minutes and repeated for three times. The FCO_2 in the water-air interface and K_{600} were calculated as described by Sawakuchi et al (2017), based on the following

10   main equation:

$$F_{CO_2} = \left(\frac{d(pCO_2)}{dt}\right)\left(\frac{V}{R \cdot T_K \cdot A}\right) \tag{1}$$

15   where d(pCO₂)/dt is the slope of the CO_2 accumulation in the chamber (µatm h⁻¹), V is the chamber volume (m³), T_K is the air temperature (in Kelvin, K), A is the surface area of the chamber at the water surface (m²), and R is the gas constant (L atm K⁻¹ mol⁻¹) (Frankignoulle, 1988).

After obtaining k, FCO_2, water and air pCO_2 accordingly to Sawakuchi et al. (2017) and normalized in K_{600} (Jahne et al., 1987; Wanninkhof, 1992; Alin et al., 2011) using the Eq. (2) and (3):

20   $$k_{600} = k_T \left(\frac{600}{Sc_T}\right)^{-0.5} \tag{2}$$

where k_T is the measured k value at *in situ* temperature (*T*), Sc_T is the Schmidt number, which can be represented by an empirical function of temperature (*T*):

$$Sc_T = 1911.1 - 118.11\,T + 3.4527\,T^2 - 0.041320\,T^3 \tag{3}$$

25   **2.2.2 Biogeochemical sampling and analysis**

In situ pH, air and water temperature were measured using a portable ORION 4-STAR meter, dissolved oxygen (DO, mg L⁻¹) and electric conductivity (µS cm⁻¹) were obtained from YSI ProODO and Amber Science 2052 meters, respectively, by continuously pumping surface water and overflowing a graduated cylinder were the probes were submerged (Ward et al., 2016). Water chemistry samples were collected from 30 cm depth using a submersible pump (Rule 360 Bilge).

Dissolved nutrients samples were filtered in 0.45 µm cellulose acetate membrane filters and preserved with thymol prior to analysis. Calcium (Ca^{2+}), magnesium (Mg^{2+}), sodium (Na^+), potassium (K^+), aluminum (Al^+), iron (Fe^+) and sulfate ($SO_4^2)^-$ ions were determined by Inductively Coupled Plasma Optical Emission Spectrometry (ICP-OES, Horiba Jobin-Yvon, model Ultima 2. NO2). Nitrate (NO_3^-), ammonium (NH_4^+), phosphate ($PO_4^+)^{-3}$ and chlorine (Cl^-) concentrations were determined

5   using a Flow Injection Analysis system (FIA, Foss Tecator, model FIASTAR 5000).

Triplicate samples were filtered through a pre-combusted GF/F filters (Whatman) into 30 mL pre-combusted glass vials with Teflon septa and preserved in the field with 30 µL of 50 % Hydrochloric acid (HCl) for determination of dissolved organic carbon (DOC), total dissolved nitrogen (TDN), dissolved organic nitrogen (DON) and dissolved inorganic nitrogen (DIN) with a Shimadzu TOC-VCPH.

10   Coarse and fine suspended sediment concentrations (CSS and FSS, respectively) were determined by filtering a known volume of water, using a churn splitter to homogenize the samples into a 0.63 µm sieve to obtain the coarse fraction and then through pre-weighted 0.45 µm cellulose acetate membrane filters to obtain the fine fraction similarly to Leite et al., (2011).

The consumption of oxygen over a 24 h period was used for the calculation of respiration rates. Three initial and final replicate samples were incubated in 60 mL acid-washed Biological Oxygen Demand bottles in the dark in river water, held at

15   ambient temperature. After these steps, oxygen concentrations were measured by Winkler Titrations method (Wetzel and Likens 1991; Ellis et al., 2012) using a Hach titrator.

2.3 Hydrodynamic and meteorological variables

Discharge, water velocity, and river depth were measured across the North Channel transect (Fig. 1) during all cruises using

20   a Sontek River Surveyor M9 Portable nine-beam 3.0 MHz/1.0 MHz/ 0.5 MHz Acoustic Doppler Current Profiler (ADCP). The precise calculation of the mean discharge, besides velocity and depth, during a complete semidiurnal tide cycle, was completed in ~ 10 to 13 hours. Normally, the net discharge measurement process requires an effort of 8 to 11 trips between the left and right banks of the Amazon River (Ward et al., 2015; Sawakuchi et al., 2017).

The meteorological data (wind speed - U_{10} and relative humidity - RH) were obtained from the National Institute of

25   Meteorology database for the nearest station (INMET station 82098, 00° 03'000" S 51°70'000" W).

2.4 Statistical analyses

To verify the normality of the data distribution the Shapiro-Wilk test was performed ($\alpha < 0.05$), in which null hypothesis of normality was rejected. Nonparametric correlation (Spearman) among FCO_2 and thermodynamic, kinetic and biogeochemical parameters were performed with a 95 % confidence interval and level of significance $\alpha < 0.05$. The Kruskal-

30   Wallis analysis (p <0.05) was performed to verify the significant differences of FCO_2, pCO_2 and net discharge for each hydrological season (high, falling, lower and rising waters). All the statistical analyzes were performed with R-project software, version3.3.2 (Develment Core Team, 2018).

3 Results

3.1 Biogeochemical and hydrodynamic seasonal variability

The regular seasons oscillation, mainly between 2014 and 2016, is shown by the annual discharge hydrograph at North

5   Channel (Fig. 2). Discharge varied from a low of nearly 33,000 m³ s⁻¹ at the end of low water season in december of 2010, to a high of about 141,000 m³ s⁻¹ in may of 2014, at the middle of high water season. At rising and high water, discharge reached $82,389 \pm 34,715$ m³ s⁻¹ and $104,637 \pm 17,505$ m³ s⁻¹ (Fig. 5), respectively. The discharge reduced roughly 50 % at low water, showing a significant variation between the seasons (Kruskal-Wallis, $p < 0.05$).

The highest CO_2 fluxes were observed during high discharge season (11.28 ± 7.82 µmol CO_2 m⁻² s⁻¹, Fig. 3). FCO_2 reached

10 24.3 µmol CO_2 m⁻² s⁻¹ in months with high discharge and was as low as 2.20 µmol CO_2 m⁻² s⁻¹ in months with low discharge, showing an expressive reduction (68 %) of the outgassing potential, with a significant seasonal variability between months with high and low discharge (Kruskal-Wallis, $p < 0.05$).

pCO_2 was higher at high water season (4575 ± 429 µatm, Fig. 3) followed by falling water (3080 ± 957 µatm, Fig. 3). During maximum discharge, the pCO_2 (4885 µatm) was about 11 times that of the concentration in the atmosphere (390 µatm,

15 Richey et al., 2002). Even at low discharge season, when the availability of organic matter related to DOC, CSS and FSS concentrations was significantly reduced (Fig. 4), the surface water pCO_2 was at least 3 times higher than the atmosphere (Fig. 3, Table 2).

The average gas exchange coefficient (K_{600}) presented high values at low and falling water (41.92 ± 5.05 cm h⁻¹ and 32.58 ± 7.2 cm h⁻¹, respectively). Wind speed showed a similar pattern with values of 2.44 ± 1.59 m s⁻¹ and 2.21 ± 0.47 m s⁻¹, for

20 falling and low water respectively (Fig. 6), with significant variability along the seasons (Kruskal-Wallis, $p < 0.005$). The highest temperatures of water and air were registered at low water (30.6 ± 0.44 °C and 29.76 ± 0.78 °C, respectively, Table 1) showing significant variability between the seasons (Kruskal-Wallis, $p < 0.01$).

NO_3^-, Al^+ and conductivity presented highest concentrations during the rising water (1.1 ± 0.36 mg L⁻¹; 0.12 ± 0.10 mg L⁻¹ and 65.87 ± 3.11 µs cm⁻¹, respectively, Table 2). The high concentration of DIN was obtained at high water (0.31 ± 0.24 mg

25 L⁻¹).

The highest pH and DO values (7.08 ± 0.38 mg L⁻¹ and 6.69 ± 0.33 mg L⁻¹) were measured at low water, when pCO_2 and FCO_2 were lowest (Table 2).

3.1 Relationship between FCO_2, pCO_2, biogeochemical and hydrodynamic variables

30 Discharge presented a positive correlation with pCO_2 (Spearman R = 0.75, $p < 0.001$, Fig. 5). But we could not find a significant correlation with FCO_2 ($p > 0.05$, Table 3).

6

The seasonal pattern of wind speed and K_{600} observed (Fig. 6) corroborated the assumptions of the expected influence of the wind on the CO_2 transfer rate in estuarine environments (Broecker and Siems, 1984; Wanninkhof 1992, Wanninkhof and McGillis 1999). However, we could not find a significant correlation between FCO_2 and wind speed ($p > 0.05$) (Table 3). Water temperature (Fig. 7) indicated a significant influence on K_{600} (Spearman R = 0.66, $p < 0.01$) and was more relevant

5   than kinetic variables (Spearman R = 0.35, $p > 0.05$), therefore being a suitable predictor variable for estimating K_{600}. A negative correlation between FCO_2, conductivity, DIN and NO_3 was observed (R = -0.43, -0.31 and -0.30 respectively, Table 3). pCO_2 presented a significant correlation with NO_3^-, DOC and Al^+ (R = -0.4, 0.41 and -0.42, respectively, Table 3). A negative correlation was registered for both pCO_2 and FCO_2 with dissolved oxygen (Table 3, Fig. 8) and pH (Table 3). Considering that a positive correlation between DOC and pCO_2 was observed, these results highlighted the influence of the

10   biological processes, especially organic matter degradation on the CO_2 outgassing (Varol and Li, 2017). On the other hand, a significant correlation between pCO_2 and respiration was not observed. This is different from what we hypothesized based in the assumption that in the river mainstem heterotrophic respiration is often considered to be a primary mechanism for aquatic CO_2 supersaturation (Mayorga et al., 2005; Ward et al., 2013).

4 Discussion

15   The highest CO_2 evasive flux and pCO_2 were observed in high discharge season. These results are consistent with previous studies in large tropical rivers (Richey et al., 2002; Li et al., 2012; Sawakuchi et al., 2017). Our observed correlations between pCO_2 and FCO_2 with DOC, air and water temperatures, pH and DO have also been shown in other tropical systems (Rasera et al., 2013; Li et al., 2012; Liu et al., 2017).

The Amazon River pCO_2 is characterize by a dynamic balance between inputs from respiration of organic matter in the
20   mainstem and floodplains and outputs from outgassing due to *in situ* primary production (Devol et al. 1987; Richey et al., 2002; Mayorga et al. 2005; Engle et al., 2008; Melack et al., 2009; Silva et al., 2009; Abril et al., 2014; Gagne-Maynard et al., 2017; Sawakuchi et al., 2017; Ward et al., 2018). This balance is directly influenced by the hydrological cycle leading to a seasonal variability of FCO_2 and pCO_2, as we observed. Rainfall is the main factor that controls the inputs of allochthonous organic matter during rising and high waters to the mainstem, while floodplains have a major role during falling water
25   season (Richey et al., 2002; Abril et al., 2014).

The higher CO_2 outgassing observed at falling water (Fig. 3) could be attributed to the influence of organic matter retention in floodplains, were intense autotrophic production occurs and when the water level start to decrease the transfer of organic matter to rivers increased (Mortillaro et al., 2012).

4.1 Biogeochemical Controls

30   The breakdown of molecules derived from terrestrial plants within the fluvial heterotrophic network is a potentially dominant source of CO_2 for the Amazon river mainstem (Duarte and Prairie, 2005; Battin et al., 2009; Abril et al., 2014,

Ward et al., 2013, 2016). As such, a positive correlation between pCO_2 and consequently FCO_2 with respiration was expected, however, this was not observed. This can be related to the bacterial growth rates, which were higher during high-rising and high-falling water than during low-rising water. Patterns of community respiration were the opposite, with respiration rates highest during low-rising water. The combination of high rates of bacterial production and low rates of

5   respiration during high water suggests that bacterial growth efficiencies were maximal during high water (Benner et al., 1995). It is important to consider, however, possible methodology inconsistences. Ward et al., (2018) showed that the titration method may lead to an underestimation of the respiration rates in the lower Amazon River, which could be the cause of the lack of correlation between these parameters. For example, it was observed that respiration rates were tightly linked to how rapidly they were mixed in carefully controlled incubation chambers and the authors further concluded that river flow

10   rates may control microbial respiration rates by controlling the suspension of sediments and particle-bound microbes (Ward et al., 2018).

The contribution of allochthonous organic matter to the river, indicated by lignin phenol compositions, has been shown to be highest during rising and high water (Ward et al., 2015), and, likewise, we registered highest concentration during high, rising and falling waters (5.02 ± 0.72 mg L^{-1}, 4.64 ± 0.6 mg L^{-1} and 4.46 ± 0.62 mg L^{-1} respectively, Table 2). At low water,

15   the DOC concentrations decreased 27 %, to 3.66 ± 0.45 mg L^{-1} (Fig. 4). These elevated DOC levels, and previously measured lignin phenols, indicate more abundant substrates for microbial decomposition, which is coincides with high pCO_2 and FCO_2.

These results indicate that most of the organic matter in the river may be carried from land to the water by lateral transport (Ward et al., 2017) and can have a strong influence on organic matter concentration in the water and consequently, how

20   terrestrial environments and floodplains may be major drivers controlling pCO_2 and FCO_2 (Mayorga et al., 2005; Ward et al., 2013, 2016, 2017; Abril et al., 2014).

The positive relationship between DOC and pCO_2 can be related to the organic carbon limited bacterial growth and respiration in whitewater rivers, Benner et al. (1995) observed that the quality of the bulk DOC is the main factor limiting bacterioplankton growth in white Amazonian rivers. The greater residence time of the water influenced by tidal cycles and

25   the influence of the flood pulse contribute to the higher concentrations of DOC at the Amazon mouth (Thomaz et al., 1998; Farjalla et al., 2002). The annual peak in high water, which typically is in June, results in the inundation of large areas of the floodplains and an accelerated exchange of materials between river and floodplains, besides the daily exchanges influenced by the tidal regime that causes a ~3 m variation in river amplitude (Benner et al., 1995; Sawakuchi et al., 2017).

Although others studies in the Amazon Basin, mainly in lakes, did not find significant correlation between DOC and pCO_2

30   (Marotta et al., 2010; Pinho et al., 2015; Valerio et al., 2018) the hydrodynamic characteristics (i.e. tidal cycle and low water velocity) and the greater bioavailability of organic matter due increased concentrations of DOC along the river continuum (Cunha et al., 2012; Seidel et al., 2015; Ward et al., 2015) create specific conditions that contribute to the heterotrophic metabolism and high concentration and evasion of CO_2 at the mouth of the Amazon River.

A negative correlation was found between FCO_2, pCO_2 and pH (Table 3). *In situ* respiration and photosynthesis can be the major drivers controlling pH at non anthropized river systems, and thus regulating the chemistry equilibrium of the dissolved inorganic carbon (DIC) system (Cole and Caraco, 2001; Rasera et al., 2013, Varol and Li, 2017). Respiration of allochthonous and autochthonous organic matter produce CO_2 that decreases pH and increase pCO_2 in the river, aquatic

5 photosynthesis increases pH and reduce dissolved CO_2 level contributing to the precipitation of carbonates (Li et al., 2012). The negative correlation between DO and CO_2 flux can be related to the oxidation of the organic matter carried out to the river (Varol and Li, 2017). In rivers, the organic matter is available in dissolved and particulate fractions, where the dissolved fraction is more easily assimilated by decomposers, while, the particulate organic matter is slowly broken down into the dissolved, through exoenzymes released by bacteria in the aquatic environment (Pusch et al., 1998). The availability

10 of DOC would control the aquatic microbial heterotrophic production, which would consequently consume O_2 and release CO_2.

FCO_2 was negatively related to conductivity, DIN and NO_3^- (Table 3). The concentrations of carbonate species (HCO_3^- and CO_3^{2-}) and some ions (Na+, Ca+, Mg+, K+ and SO_4^2) determines the conductivity in the aquatic environment, which were observed with highest concentrations during the rising and low water, which could be related to the influence of groundwater

15 and lower dilution capacity due discharge reduction (Neiff, 1990; Thomaz et al., 2007; Silva et al., 2013; Cunha and Sternberg, 2018). NO_3^- concentrations showed the same pattern, considering that increasing nitrogen could elevate aquatic photosynthesis and reduce pCO_2, limitation of bacterial growth by nitrogen and organic carbon was also observed in some freshwater ecosystems (Wang et al., 1992; Benner et al., 1995; Elser et al., 1995; Li et al., 2012). During the low water the CSS and FSS concentrations decreased 55 % and 33 %, respectively, which could be related to the limited floodplain

20 connectivity, promoting the higher light input in the water column (Gagne-Maynard et al., 2017).

4.2 Hydrodynamic and Meteorological Controls

As observed in our study, pCO_2 had a strong and positive correlation with discharge (R = 0.75, p <0.01, Fig. 5) and a negatively correlation with water temperature (R = -0.68, p <0.01). The pCO_2 can be influenced by rainfall intensity, flood

25 pulse and river discharge that controls the input of organic matter in river system (Finlay, 2003). In addition, the combination of hydrodynamic and meteorological parameters, such as water velocity, water temperature and wind speed determine the air-water turbulence which controls the CO_2 outgassing (Barth and Veizer, 1999; Alin et al., 2011).

The local precipitation in the basin added to the upstream hydrological characteristics (geomorphology, size, relief, slope of the channel, land and soil cover use, etc) regulate the net discharge in a certain stretch of the river. In turn, depending on the

30 characteristics of the water body (river, estuary, lake), there may be interactions between the wind and the surface of the water, generating more turbulence and promoting synergistic effects that tend to increase the mass transfer coefficient in the air-water interface, consequently, these interactions increase the CO_2 outgassing (Alin et al., 2011; Varol and Li, 2017). However, this relation between water velocity and FCO_2 was not observed in the studied site near the Amazon River mouth

due the lower water velocity (roughly 0.7 m s^{-1}, Table 1) in comparison to upstream sections of the Amazon, where no tidal effect is present, i.e. Óbidos with 1.92 m s^{-1} (Sawakuchi et al., 2017).

Our results showed that water and air temperature presented a strong influence on FCO$_2$ (Table 3) and K$_{600}$ (Fig. 8). As observed in other tropical rivers (Li et al., 2012, Liu et al., 2017) the mean water temperature is considered relatively high at the Amazon River (Moreira-Turcq, 2013). Thus, water temperature and turbulence, both factors can reduce the gases solubility in the water leading to a higher exchange ratio (for instance, CO$_2$ and DO) and in addition accelerating the decomposition of organic matter (Alin et al., 2011, Li et al., 2012, Ward et al., 2018).

In estuaries wind speed is often the major source of turbulence on the water surface (Alin et al., 2011). A high rate of gaseous transfer, at any wind speed, can be favored when both wind and water currents have opposing directions. These effects result in the sum of both velocities and, consequently, tend to intensify the level of turbulence at the interface air-water (Zappa et al., 2007; Beaulieu et al., 2012; Sawakuchi et al., 2017). However, the absence of correlation with U$_{10}$ and FCO$_2$ in our investigation may be explained by the use of wind velocity data, obtained from weather stations located on land relatively far from sampling points, leading to the use of possible non-representative data.

5 Conclusion

Higher pCO$_2$ and CO$_2$ outgassing were observed during the high waters season highlight the strong influence of the hydrological cycle. This coincides with the peaks of dissolved organic matter concentration, water and air temperature contributing to the increase in pCO$_2$.

 These assumptions are confirmed by the positive correlation between FCO$_2$ and pCO$_2$ with DOC, and negative correlation with water and air temperatures. Consequently, these variables could be considered suitable predictors for estimating pCO$_2$ and FCO$_2$ in the Amazon River mouth area. For a better estimation and understanding of carbon budgets in tropical rivers it is still required to verify and to quantify more deeply the relationship among CO$_2$ evasion and others hydrodynamic, meteorological and biogeochemical variables. Our results can support the development, adjustment and parameterization of regional models of CO$_2$ emissions in the study area, providing a significant contribution for the understanding of carbon cycle of the Amazon River mouth, reducing the FCO$_2$ estimates errors for different temporal scales in large tropical rivers.

Author contributions

DL, HS, VN, AV, WG, DB, CA and JD executed in situ measurements and laboratory procedures. DL, DB, HS and VN developed the data calculation and interpretation JR, AK, HS, NW, AC and DB organized overall project logistics, and local laboratory support. The manuscript was prepared by DL and all the authors discussed/commented/ revised the manuscript and approved the final submission.

5 **Acknowledgments**

10

Competing interests

The authors declare that they have no conflict of interest.

References

Abril, G., Martinez, J. M., Artigas, L. F., Moreira-Turcq P., Benedetti, M F., Vidal L., Meziane, T., Kim, J. H.,Bernardes, M.
15 C., Savoye, N., Deborde, J., Souza, E. L., Albéric, P., Souza, M . F. L., and Roland, F.: Amazon River carbon dioxide outgassing fuelled by wetlands, Nature, 505, 395–398, doi:10.1038/nature12797, 2014.

Alin, S. R., Rasera, M. F. F. L., Salimon, C. I., Richey, J. E., Holtgrieve, G. W., Krusche, A. V. and Snidvongs, A: Physical controls on carbon dioxide transfer velocity and flux in low gradient river systems and implications for regional carbon
20 budgets, Journal of Geophysical, 116 (G01009), 1-17, doi:10.1029/2010JG001398, 2011.

Aufdenkampe, A. K., Mayorga, E., Raymond, P. A., Melack, J. M., Doney, S. C., Alin, S. R., Aalto, R. E.,and Yoo, K.: Riverine coupling of biogeochemical cycles between land, oceans, and atmosphere, Frontiers in the Ecology and Environment, 9, 53–60, doi:10.1890/100014, 2011.

25

Barth, J. A. C., Veizer, J. A.: Carbon cycle in St. Lawrence aquatic ecosystems at Cornwall (Ontario), Canada: seasonal and spatial variations, Chemical Geology, 159, 107-128, doi: 10.1016/S0009-2541(99)00036-4, 1999.

Battin, T. J., Kaplan, L. A., Findlay, S., Hopkinson, C. S., Marti, E., Packman, A. I., Newbold, D., and Sabate, F.:
30 Biophysical controls on organic carbon fluxes in fluvial networks, Nature Geoscience, 1, 95–100, doi:10.1038/ngeo101, 2009.

Beaulieu, J. J., Shuster, W. D., and Rebholz, J. A.: Controls on gas transfer velocities in a large river, Journal of Geophysical Research Biogeosciences, 117, G02007, doi: 10.1029/2011jg001794, 2008, 2012.

Benner, R., Opsahl, S., Chin-Leo, G., Richey, J. E., and Forsberg, B. R.: Bacterial carbon metabolism in the Amazon River
5 system, Limnology and Oceanography, 40, 1262–1270, doi:10.4319/lo.1995.40.7.1262, 1995.

Borges, A. V., Vanderborght, J. P., Schiettecatte, L. S., Gazeau, F., Ferron-Smith, S., Delille, B. and Frankignoulle, M.: Variability of the gas transfer velocity of CO_2 in a macrotidal estuary (the Scheldt), Estuaries, 27, 593–603, doi: 10.1007/bf02907647, 2004.

10

Brienen, R. J. W., Phillips, O. L., Feldpausch, T. R., Gloor, E., Baker, T. R., Lloyd, J., Lopez-Gonzalez, G., Mendoza, A., Lewis, S. L., Vásquez Martinez, R., Alexiades, M., Álvarez Dávila, E., Alvarez-Loayza, P., Andrade, A., Aragão, L. E. O. C., Araujo-Murakami, A., Arets, E. J. M. M., Arroyo, L., Aymard C., G. A., Bánki, O. S., Baraloto, C., Barroso, J., Bonal, D., Boot, R. G. A., Camargo, J. L. C., Castilho, C. V., Chama, V., Chao, K. J., Chave, J., Comiskey, J. A., Cornejo Valverde,
15 F., da Costa, L., de Oliveira, E. A., Di Fiore, A., Erwin, T. L., Fauset, S., Forsthofer, M., Galbraith, D. R., Grahame, E. S., Groot, N., Hérault, B., Higuchi, N., Honorio Coronado, E. N., Keeling, H., Killeen, T. J., Laurance, W. F., Laurance, S., Licona, J., Magnussen, W. E., Marimon, B. S., Marimon-Junior, B. H., Mendoza, C., Neill, D. A., Nogueira, E. M., Núñez, P., Pallqui Camacho, N. C., Parada, A., Pardo-Molina, G., Peacock, J., Peña-Claros, M., Pickavance, G. C., Pitman, N. C. A.Poorter, L., Prieto, A., Quesada, C. A., Ramírez, F., Ramírez-Angulo, H., Restrepo, Z., Roopsind, A., Rudas, A., Salomão,
20 R. P., Schwarz, M., Silva, N., Silva-Espejo, J. E., Silveira, M., Stropp, J., Talbot, J., ter Steege, H., Teran-Aguilar, J., Terborgh, J., Thomas-Caesar, R., Toledo, M., Torello-Raventos, M., Umetsu, R. K., van der Heijden, G. M. F., van der Hout, P., Guimarães Vieira, I. C., Vieira, S. A., Vilanova, E., Vos, V. A., Zagt, R. J.: Long-term decline of the Amazon carbon sink, Nature, 519, doi:10.1038/nature14283, 2015.

25

Broecker, H. C. and Siems, W.: The role of bubbles for gas transfer from water to air at higher wind speeds: experiments in wind-wave facility in Hamburg, In Gas Transfer at Water Surfaces, Eds. W. Brutsaert and G. H. Jirka, p. 229–238. Reidel, Dordrecht: The Netherlands, 1984.

30 Cole, J. J. and Caraco, N. F.: Carbon in catchments: connecting terrestrial carbon losses with aquatic metabolism, Marine and Freshwater Research, 52, 101–110, https://doi.org/10.1071/MF00084, 2001.

Cole, J. J., Prairie, Y. T., Caraco, N. F., McDowellL, W. H., Tranvik, J., Striegl R. G., Duarte, C. M., Kortelainen, P. Downing, J. A., Middelburg, J. J. and Melack, J.: Plumbing the Global Carbon Cycle: Integrating Inland Waters into the Terrestrial Carbon Budget, Ecosystems, 10, 172–185, https://doi.org/10.1007/s10021-006-9013-8, 2007.

Costa, A. C. L., Silva Junior, A. A., Cunha, A. C., Galbrarth, D., Feitosa, J. R. P. and Mattos, A.: Distribuição geoespacial e
5   horária da temperatura do ar na cidade de Belém-PA, Brazilian Geographical Journal, 4, 150-168, 2013.

Cunha, A. C., Brito, D. C., Brasil Junior, A. C., Pinheiro, L. A. R., Cunha, H. F. A. and Krusche, A. V.: Challenges and Solutions for Hydrodynamic and Water Quality in Rivers in the Amazon Basin, In Hydrodinamics: Natural Water Bodies , Eds. H. Ed. Schulz; A. L. A. Simões; R. J, Rijeka: InTech - Croacia, p. 67-88, 2012, doi 10.5772/27796

10 Cunha, A. C. and Sternberg, L. S. L.: Using stable isotopes ^{18}O and ^{2}H and biogeochemical analysis to identify factors affecting water quality in four estuarine Amazonian shallow lakes, Hydrological Processes, v. 32, p. 1188-1201, 2018 https://doi.org/10.1002/hyp.11462.

Devol, A. H., Quay, P. D. and Richey, J. E.: The role of gas exchange in the inorganic carbon, oxygen, and 222Rn budgets
15 of the Amazon River, Limnology and Oceanography, 32, 235–248, doi: 10.4319/lo.1987.32.1.0235. 32: 235–248, 1987.

Duarte, C. M. and Prairie, Y. T.: Prevalence of heterotrophy and atmospheric CO_2 emissions from aquatic ecosystems. Ecosystems, 8, 862–870, https://doi.org/10.1007/s10021-005-0177-4, 2005.

20 Ellis, E. E., Richey, J. E., Aufdenkampe, A. K., Krusche, A.V., Quay, P. D., Salimon C., and da Cunha, H. B.: Factors controlling water-column respiration in rivers of the central and southwestern Amazon Basin, Limnology and Oceanography, 57, doi: 10.4319/lo.2012.57.2.0527, 2012.

Elser, J. J., L. B. Stabler, L. B., and Hassett, R. P. 1995.: Nutrient limitation of bacterial growth and rates of bacterivory in
25 lakes and oceans: a comparative study, Aquatic Microbial Ecology, 9, 105–110, doi: 10.3354/ame00910, 1995.

Engle, D. L., Melack, J. M., Doyle, R. D. and Fisher, T. R.: High rates of net primary production and turnover of floating grasses on the Amazon floodplain: implications for aquatic respiration and regional CO_2 flux, Global Change Biology, 14, 369–381, doi: 10.1111/j.1365-2486.2007.01481.x, 2008.
30

Farjalla, V. F., Esteves, F. A., Bozelli, R. L., Roland, F.: Nutrient limitation of bacterial production in clear water Amazonian ecosystems, Hydrobiologia, 489, 197–205, doi: 10.1023/A:1023288922394, 2002.

Finlay, J. C.: Controls of streamwater dissolved inorganic carbon dynamic in a forest watershed, Biogeochemistry, 62, 231-252, doi 10.1023/A:1021183023963, 2003.

5   Frankignoulle, M.: Field-measurements of air sea CO_2 exchange, Limnology and Oceanography, 33, 313-322, doi: 10.4319/lo.1988.33.3.0313, 1988.

Frankignoulle, M. Borges, A. and Biondo, R.: A new design of equilibrator to monitor carbon dioxide in highly dynamic and turbid environments, Water Research, 35, 1344-1347, doi 10.1016/S0043-1354(00)00369-9, 2001.

10

Gagne-Maynard, W. C., Ward, N. D., Keil, R. G., Sawakuchi, H. O., Da Cunha, A. C., Neu, V., Brito, D. C., Krusche, A. V and J. E. Richey.: Evaluation of primary production in the lower Amazon River based on a dissolved oxygen stable isotopic mass balance, Frontiers in Marine Science, 4, 1–12, doi: https://doi.org/10.3389/fmars.2017.00026, 2017.

15   Goes, J. I., Gomes, H. R., Chekalyuk, A. M., Carpenter, E. J.,. Montoya, J. P., Coles, V. J.. Yager, P. L., Berelson, W. M., Capone, D. G.,   Foster, R. A., Steinberg, D. K., Subramaniam, A., Hafez, M. A.: Influence of the Amazon River discharge on the biogeography of phytoplankton communities in the western tropical north Atlantic, Progress in Oceanography, 120, 29-40, doi: 10.1016/j.pocean.2013.07.010, 2014.

20   Hedges, J. I., Clark, W. A., Quay, P. D., Richey, J. E., Devol, A. H. and Santos, M.: Compositions and fluxes of particulate organic material in the Amazon River, Limnology and Oceanography, 4, doi: 10.4319/lo.1986.31.4.0717, 1986.

Hedges, J. I., Mayorga, E., Tsamakis E., McClain, M. E., Aufdenkampe, A., Quay, P., Richey, J. E., Benner, R., Opsahl, S., Black, B., Pimentel, T., Quintanilla, J. and Maurice, L.: Organic matter in Bolivian tributaries of the Amazon River: A
25   comparison to the lower mainstream, Limnology and Oceanography, 7, doi: 10.4319/lo.2000.45.7.1449, 2000.

INMET- Instituto Nacional de Meteorologia, Historical average of Precipitation (1981 to 2010), Available at: http://www.inmet.gov.br/portal/index.php?r=clima/normaisclimatologicas.

30   Jahne, B., Munnich, K. O., Bosinger, R., Dutzi, A., Huber,W., and Libner, P.: On the parameters influencing air-water gas exchange, Journal of Geophysical Research, Oceans, 92, 1937–1949, doi: 10.1029/JC092iC02p01937, 1987.

Köppen, W: Climatologia: non un estudio de los climas de la tierra, México: Fondo de Cultura Econômica, 1948, 463p.

Leite, N. K., Krusche, A.V., Ballester, M.V.R.,Victoria, R. L., Richey, J. E. and Gomes, B. M: Intra and interannual variability in the Madeira River water chemistry and sediment load, Biogeochemistry, 105, 37–51, https://doi.org/10.1007/s10533-010-9568-5, 2011.

5   Le Quéré, C., Moriarty, R., Andrew, R. M., Peters, G. P., Ciais, P., Friedlingstein, P., Jones, S. D., Sitch, S., Tans, P., Arneth, A., Boden, T. A., Bopp, L., Bozec, Y., Canadell, J. G., Chini, L. P., Chevallier, F., Cosca, C. E., Harris, I., Hoppema, M., Houghton, R. A., House, J. I., Jain, A. K., Johannessen, T., Kato, E., Keeling, R. F., Kitidis, V., Klein Goldewijk, K., Koven, C., Landa, C. S., Landschützer, P., Lenton, A., Lima, I. D., Marland, G., Mathis, J. T., Metzl, N., Nojiri, Y., Olsen, A., Ono, T., Peng, S., Peters, W., Pfeil, B., Poulter, B., Raupach, M. R., Regnier, P., Rödenbeck, C., Saito, S., Salisbury, J.
10 E., Schuster, U., Schwinger, J., Séférian, R., Segschneider, J., Steinhoff, T., Stocker, B. D., Sutton, A. J., Takahashi, T., Tilbrook, B., van der Werf, G. R., Viovy, N., Wang, Y.-P., Wanninkhof, R., Wiltshire, A., and Zeng, N.: Global carbon budget 2014, Earth System Science Data, 7, 47-85, https://doi.org/10.5194/essd-7-47-2015, 2015.

Li, S., Lu, X. X., M, He., Zhou, Y., Li, L. and Zieglerc, A. D: Daily CO_2 partial pressure and CO_2 outgassing in the upper
15 Yangtze River basin: A case study of the Longchuan River, China, Journal of Hydrology, 466–467, 141–150, https://doi.org/10.1016/j.jhydrol.2012.08.011, 2012.

Liu, S., Lua, X. X., Xia, X., Yang, X. and Ran, L.: Hydrological and geomorphological control on CO_2 outgassing from low-gradient large rivers: An example of the Yangtze River system, Journal of Hydrology, 550, 26–41,
20 http://dx.doi.org/10.1016/j.jhydrol.2017.04.044, 2017.

Mayorga, E., Aufdenkampe, A. K., Masiello, C. A., Krusche, A. V., Hedges, J. I., Quay, P. D., Richey, J. E., and Brown, T. A.: Young organic matter as a source of carbon dioxide outgassing from Amazonian rivers, Nature, 436, 538–541, doi: 10.1038/nature03880, 2005.

25
Marotta, H., Duarte, C. M., L Pinho, L. and Enrich-Prast, A.: Rainfall leads to increased pCO_2 in Brazilian coastal lakes, Biogeosciences, 7, 5, 1607–1614, doi: 10.5194/bg-7-1607-2010, 2010.

Melack, J. M., Novo, E. M. L. M., Forsberg, B. R., Piedade, M. T. F. and L. Maurice, L. Floodplain ecosystem processes, In:
30 'Amazonia and Global Change', Eds. Gash, J., Keller, M. and Silva-Dias, P., pp. 525–541, American Geophysical Union: Washington, USA, 2009.

Molinas, E., Vinzon, S. B., de Paula Xavier Vilela, C. and Gallo, M. N. Structure and position of the bottom salinity front in the Amazon Estuary, Ocean Dynamics, 64, 1583–1599, https://doi.org/10.1007/s10236-014-0763-0, 2014.

Molinier M., Guyot J. L., Oliveira E., and Guimaraes V.: Les regimes hydrologiques de l'Amazone et de ses affluents, In: 'L'hydrologie tropicale: geoscience et outil pour le developpement', Eds. Chevallier, P. and Pouyaud, B., pp. 209-222, AIHS: Paris, France, 1996.

5

Moreira-Turcq, P., Seyler, P., Guyot, J. L. and Etcheber, H.: Exportation of organic carbon from the Amazon River and its main tributaries, Hydrology Processes, 17, 1329–1344, doi:10.1002/hyp.1287, 2003.

Moreira-Turcq, P., Bonnet, M.-P., Amorim, M.; Bernardes, M., Lagane, C., Maurice, L., Perez, M., and Seyler, P.:
10 Seasonal variability in concentration, composition, age, and fluxes of particulate organic carbon exchanged between the floodplain and Amazon River, Global Biogeochemestry Cycles, 27, 119–130, doi:10.1002/gbc.20022, 2013.

 Mortillaro, J-M., Rigal F., Rybarczyk H., Bernardes M., Abril G., Meziane T.: Particulate Organic Matter Distribution along the Lower Amazon River: Addressing Aquatic Ecology Concepts Using Fatty Acids, Plos One, 7, 1-10,
15 doi:10.1371/journal.pone.0046141, 2012.

Neiff, J. J.: Ideas para la interpretación ecológica del Paraná, Interciencia, 15, 424–44, 1990.

Pinho, L., Duarte, C. M., Marotta, H. and Enrich-Prast, A.: Temperature-dependence of the relationship between pCO$_2$ and
20 dissolved organic carbon in lakes, Biogeosciences, 12, 3, 2787–2808, doi:10.5194/bg-13-865-2016, 2016.

Pusch, M., Fiebig, D., Brettar, I., Eisenmann, H., Ellis, B. K., Kaplan, L. A., Lock, M. A., Naegeli, M. W. and Traunspurger, W.: The role of micro-organisms in the ecological connectivity of running waters, Freshwater Biology, 40, 453–495, doi:10.1046/j.1365-2427.1998.00372.x, 1998.

25

R Development Core Team.: 'R: A language and environment for statistical computing, reference index version 2.12.1', Vienna: R Foundation for Statistical Computing, ISBN 3-900051-07-0, 2014, Avaliable at   http://www.R-project.org [accessed January 2018], 2018.

30 Rasera, M. F. F. L., Ballester, M. V. R., Krusche, A. V., Salimon, C., Montebelo, L. A., Alin, S. R., Victoria, R. L. and Richey, J. E.: Estimating the Surface Area of Small Rivers in the Southwestern Amazon and Their Role in CO$_2$ Outgassing, Earth Interactions, 12, 1-16, https://doi.org/10.1175/2008EI257.1, 2008.

Rasera, M. F. F. L., Krusche, A. V., Richey, J. E., Ballester, M. V. R., and Victória, R. L. Spatial and temporal variability of pCO_2 and CO_2 efflux in seven Amazonian Rivers, Biogeochemistry, 116, 241–259, doi: 10.1007/s10533-013-9854-0, 2013.

Raymond, P. A. and Cole, J. J.: Gas Exchange in Rivers and Estuaries: Choosing a Gas Transfer Velocity, Estuaries 24, 312–
5 317, http://www.jstor.org/stable/1352954, 2001.

Richey, J. E., Meade, R. H., Salati, E., Devol, A. H., Nordin Jr., C. F. and Santos, U. D.: Water Discharge and Suspended Sediment Concentrations in the Amazon River: 1982–1984, Water Resources Research, 22, 756–764, doi:10.1029/WR022i005p00756, 1986.

10

Richey, J. E., Hedges, J. I., Devol, A. H., Quay, P. D., Victoria, R., Martinelli, L. and Forsberg, B. R.: Biogeochemistry of carbon in the Amazon River, Limnology and Oceanography, 35, doi: 10.4319/lo.1990.35.2.0352, 1990.

Richey, J. E., Melack, J. M., Aufdenkampe, A. K., Ballester, V. M., and Hess, L. L.: Outgassing from Amazonian rivers and
15 wetlands as a large tropical source of atmospheric CO_2, Nature, 416, 617–620, doi: 10.1038/416617a, 2002.

Richey, J. E.: Pathways of atmospheric CO_2 through fluvial systems, In: The Global Carbon Cycle: Integrating Humans, Climate, and the Natural World, Eds Field, C.B., Raupach, M.R, pp. 329–340, Island Press: Washington, USA, 2003.

20 Sawakuchi H. O., Neu, V., Ward, N. D., Barros, M. L. C., Valerio, A. M., Gagne-Maynard, W., Cunha, A. C., Less, D. F. S., Diniz J. E. M., Brito, D. C., Krusche Alex V. and Richey, J. E.: Carbon Dioxide Emissions along the Lower Amazon River, Frontiers in Marine Science, 4, Doi: 0.3389/fmars.2017.00076, 2017.

Seidel, M., Yager, P. L., Ward, N. D., Carpenter, E. J., Gomes, H. R., Krusche, A. V., Richey. J. E., Dittmarb, T. and
25 Medeiros, P. M.: Molecular-level changes of dissolved organic matter along the Amazon River-to-ocean continuum, Marine Chemistry, 177, 218–231, doi: 10.1016/j.marchem.2015.06.019, 2015.

Silva, T. S. F., Costa, M. P. F. and Melack, J. M.: Annual net primary production of macrophytes in the eastern Amazon floodplain, Wetlands, 29, 747–758, doi: doi.org/10.1672/08-107.1, 2009.

30

Silva, M. T., Pereira, J. O., Vieira, L. J. S. and Petry, A. C.: Hydrological seasonality of the river affecting fish community structure of oxbow lakes: A limnological approach on the Amapá Lake, southwestern Amazon, Limnologica, 43, 79–90, http://dx.doi.org/10.1016/j.limno.2012.05.002, 2013.

Thomaz, S. M., Bini, L. M. and Bozelli, R. L. Floods increase similarity among aquatic habitats in river-floodplain systems, Hydrobiologia, 579, 1–13, https://doi.org/10.1007/s10750-006-0285-y, 2007.

Valerio, A. M., Kampel, M., Vantrepotte, V., Ward, N. D., Sawakuchi, H. O., Less, D. F. S., Neu, V., Cunha, A. and Richey, J.: Using CDOM optical properties for estimating DOC concentrations and pCO_2 in the Lower Amazon River, Optical Express, 26, A657-A677, https://doi.org/10.1364/OE.26.00A657, 2018.

Varol, M., and Li, S.: Biotic and abiotic controls on CO_2 partial pressure and CO_2 emission in the Tigris River, Turkey, Chemical Geology, 449, http://dx.doi.org/10.1016/j.chemgeo.2016.12.003, 2017.

Wang, L., Miller, T. D., and Priscu, J. C. Bacterioplankton nutrient deficiency in a eutrophic lake. Archiv fur Hydrobiologie, 125, 423–439, 1992.

Wanninkhof, R.: Relationship between wind speed and gas exchange over the ocean, Journal of Geophysical Research, 97, 7373–7382, doi:10.1029/92JC00188, 1992.

Wanninkhof, R. and W. R. McGillis.: A cubic relationship between air-sea CO_2 exchange and wind speed, Geophysical Research Letters, 26, 1889–1892, doi: 10.1029/1999GL900363, 1999.

Ward, N. D., Keil, R. G., Medeiros, P. M., Brito, D. C., Cunha, A. C., Dittmar, T., Yager, P. L., Krusche, A. V. and Richey, J. E.: Degradation of terrestrially derived macromolecules in the Amazon River, Nature Geoscience, 6, 530-533, doi:10.1038/ngeo1817, 2013.

Ward, N. D., Krusche, A. V., Sawakuchi, H. O., Brito, D. C., Cunha, A. C., Moura, J. M. S., da Silva, R., Yager, P. L., Keil, R. G. and Richey, J. E.: The compositional evolution of dissolved and particulate organic matter along the lower Amazon River-Óbidos to the ocean, Marine Chemistry, 177, 244–256, doi.org/10.1016/j.marchem.2015.06.013, 2015.

Ward, N. D., Sawakuchi, H. O., Gagne-Maynard, W., Cunha, A. C., Brito, D. C., Neu, V., Valerio, A. M., Silva, R., Krusche, A. V., Richey, J. E. and Keil, R. G.: The reactivity of plant-derived organic matter and the potential importance of priming effects along the lower Amazon River, Journal of Geophysical Research-Biogeosciences, 121, 1522-1539, doi: 10.1002/2016JG003342, 2016.

Ward, N. D., Sawakuchi, H. O., Neu, V., Less, D. F. S, Valerio, A. M., Cunha, A. C. , Kampel, M., Bianchi, T. S., Krusche, A. V., Richey, J. E., and Keil, R. G.: Velocity-amplified microbial respiration rates in the lower Amazon River, Limnology and Oceanography, 00, 1-10, doi: 10.1002/lol2.10062, 2018.

5 Wetzel, R. G., and Likens, G. E.: 'Limnological analyses', 2nd Edn. Springer-Verlag: Berlin, Germany, 1991.

Yao, G., Gao, Q., Wang, Z., Huang, X., He, T.,Zhang, Y., Jiao, S., Ding, J.: Dynamics of CO_2 partial pressure and CO_2 outgassing in the lower reaches of the Xijiang River, a subtropical monsoon river in China, Science of The Total Environment, 376, 255-266, doi: 10.1016/j.scitotenv.2007.01.080, 2007.

10

Zappa, C. J., McGillis, W. R., Raymond, P. A., Edson, J. B., Hintsa, E. J., Zemmelink, H. J., Dacey, J. W. H and Ho, D. T.: Environmental turbulent mixing controls on air-water gas exchange in marine and aquatic systems, Geophysical Research Letters, 34, L10601, doi: 10.1029/2006gl028790, 2007.

Table 1: Hydrodynamics, kinetic and meteorological variables according to the season (mean ± standard deviation).

Sampling Season	Discharge (m³ s⁻¹)	Wind speed (m s⁻¹)	Water velocitiy (m s⁻¹)	Depht (m)	Water temperature (°C)	Air temperature (°C)	Relative Humidity (%)	Gas Transfer Velocity (cm h⁻¹)
Rising	82389 ± 34715	1.05 ± 0.39	0.82 ± 0.29	24.26	28.53 ± 0.74	27.31 ± 1.07	87 ± 9	25.15 ± 5.76
High	104637 ± 17505	1.54 ± 1.25	0.65 ± 0.20	18.37 ± 0.18	28.86 ± 0.47	28.25 ± 1.81	79 ± 12	31.14 ± 14.49
Falling	064 ±19743	2.44 ± 1.59	0.63 ± 0.26	18.22 ± 0.73	29.71 ± 0.47	28.17 ± 0.90	69 ± 12	32.58 ± 7.2
Low	52978 ± 8875	2.21 ± 0.47	0.69 ± 0.32	17.98 ± 0.14	30.6 ± 0.44	29.76 ± 0.78	69 ± 11	41.92 ± 4.77

Table 2: Biogeochemical parameters according to the season (mean ± standard deviation).

Sampling Season	FCO_2 (µmol m⁻² s⁻¹)	pCO_2 (µatm)	Eletric Conductivity (µs cm⁻¹)	DO (mg L⁻¹)	pH	NO_3^- (mg L⁻¹)
Rising	5.46 ± 2.18	2127 ± 530	65.87 ± 3.11	6.13 ± 0.44	6.8 ± 0.42	1.13 ± 0.22
High	10.55 ± 6.27	4575 ± 429	53.42 ± 5.90	4.56 ± 0.38	6.42 ± 0.48	0.95 ± 0.4
Falling	11.28 ± 7.82	3080 ± 957	48.78 ± 4.46	5.33 ± 0.66	6.56 ± 0.3	0.73 ± 0.33
Low	3.56 ± 1.14	1322 ± 255	65.74 ± 0.67	6.69 ± 0.33	7.08 ± 0.38	1.1 ± 0.36

Sampling Season	FSS (mg L⁻¹)	CSS (mg L⁻¹)	DOC (mg L⁻¹)	Respiration (µmol h⁻¹)	Al^+ (mg L⁻¹)	DIN (mg N L⁻¹)
Rising	104.95 ± 62.94	1.47 ± 1.31	4.64 ± 0.6	0.77 ± 0.96	0.12 ± 0.10	0.29 ± 0.05
High	87.65 ± 55.89	0.99 ± 1.33	5.02 ± 0.72	0.21 ± 0.18	0.07 ± 0.03	0.31 ± 0.24
Falling	56.08 ± 46.83	1.83 ± 2.46	4.46 ± 0.62	0.55 ± 0.59	0.08 ± 0.05	0.21 ± 0.09
Low	59.51 ± 51.92	0.45 ± 0.34	3.66 ± 0.45	0.46 ± 0.35	0.03 ± 0.03	0.29 ± 0.14

Table 3: Significative Spearman correlation between FCO$_2$, pCO$_2$, biogeochemical, hydrodynamic and meteorological variables.

	pCO$_2$	Eletric Conductivity	DO	pH	NO$_3^-$	DIN	DOC	Respiration	Al$^+$	Q	Depht	Water temperature	Air temperature	RU	K$_{600}$
FCO$_2$	0.66	-0.43	-0.55	-0.49	-0.30	-0.31	0.39	-0.08	-0.17	0.20	0.03	-0.30	-0.43	-0.04	-0.28
p-value	<0.01	<0.05	<0.01	<0.01	<0.05	<0.05	<0.01	>0.05	>0.05	>0.05	>0.05	<0.01	<0.01	>0.05	>0.05
pCO$_2$	-	-0.31	-0.93	-0.42	-0.40	-0.26	0.41	-0.36	-0.42	0.75	-0.38	-0.68	-0.63	0.40	-0.51
p-value	-	>0.05	<0.01	<0.05	<0.05	>0.05	<0.05	0.09	<0.05	<0.01	0.05	<0.01	<0.01	<0.05	<0.01
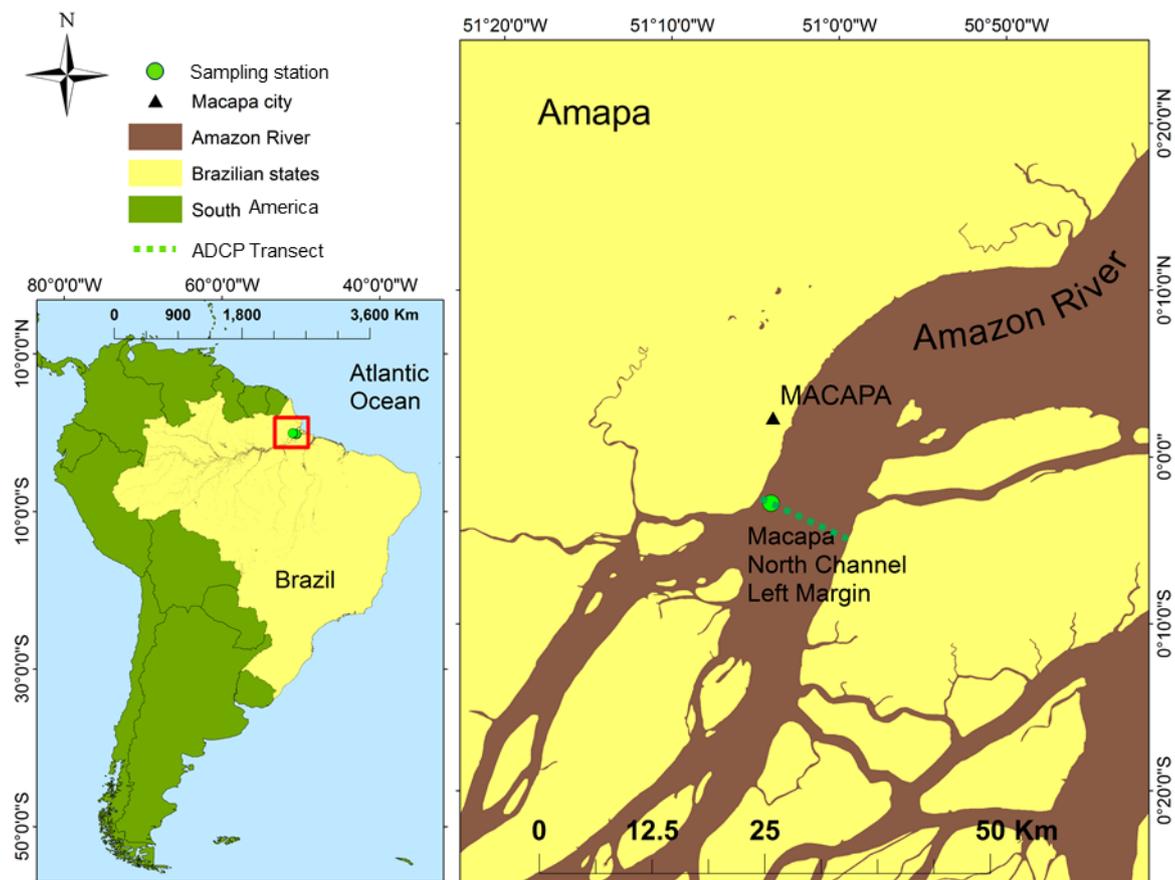
Figure 1: Study area and location of sampling key-station at left margin of North channel (S 00°02'872'' W 051°04'616'').
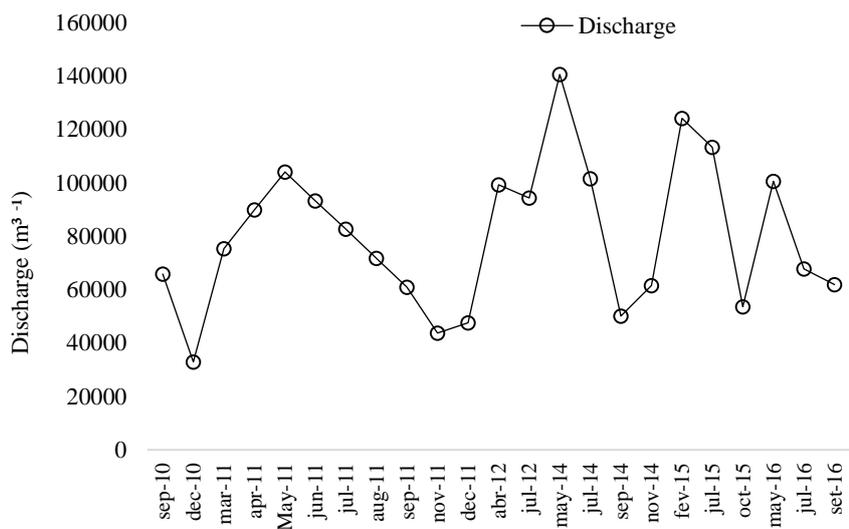
Figure 2: Discharge at North Channel with open cycles showing the data of time series samplings.
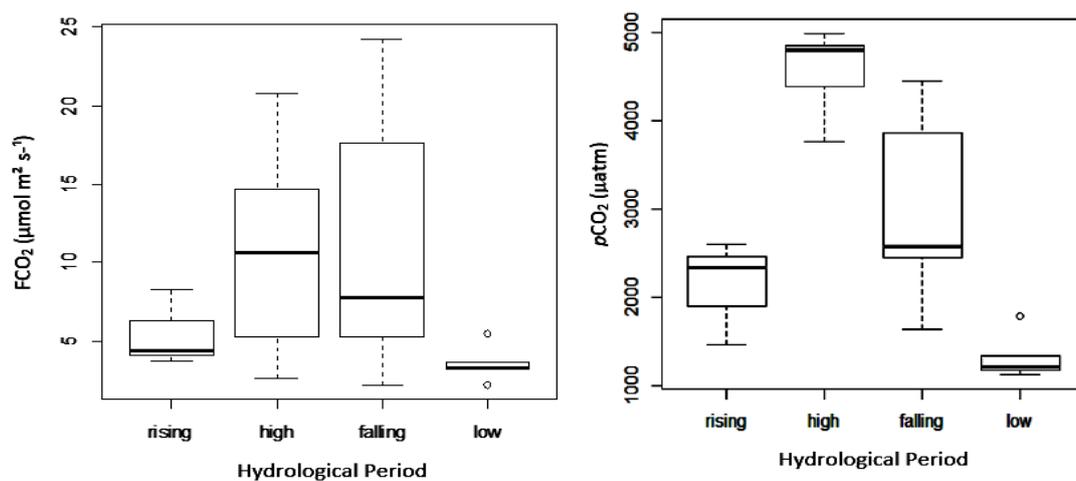
5

Figure 3: Seasonal variability of FCO₂ and pCO₂.
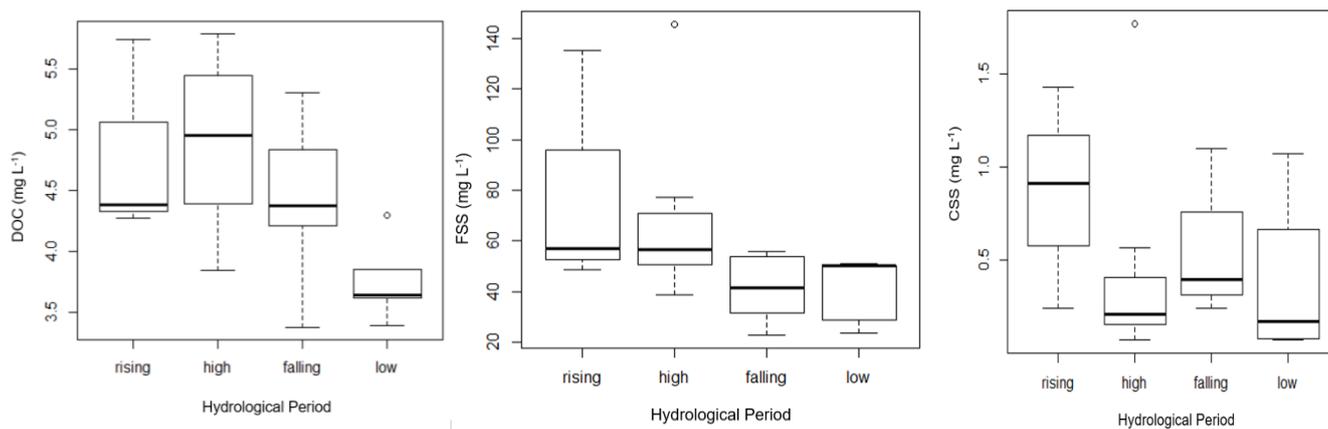
Figure 4: Seasonal variability of DOC, FSS and CSS.

5
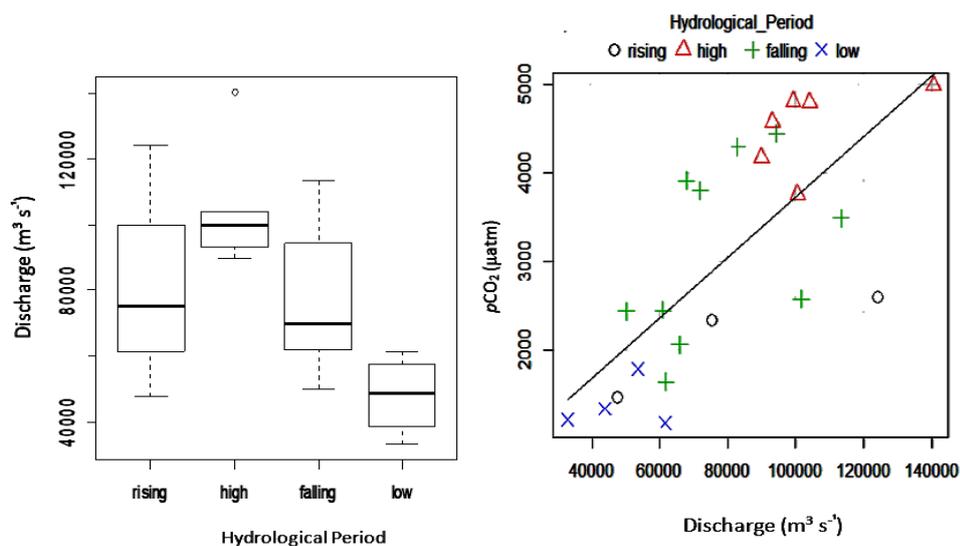
Figure 5: Seasonal variability of discharge and the relation between Q x pCO$_2$ (R^2 =0.47, p < 0.001).

10
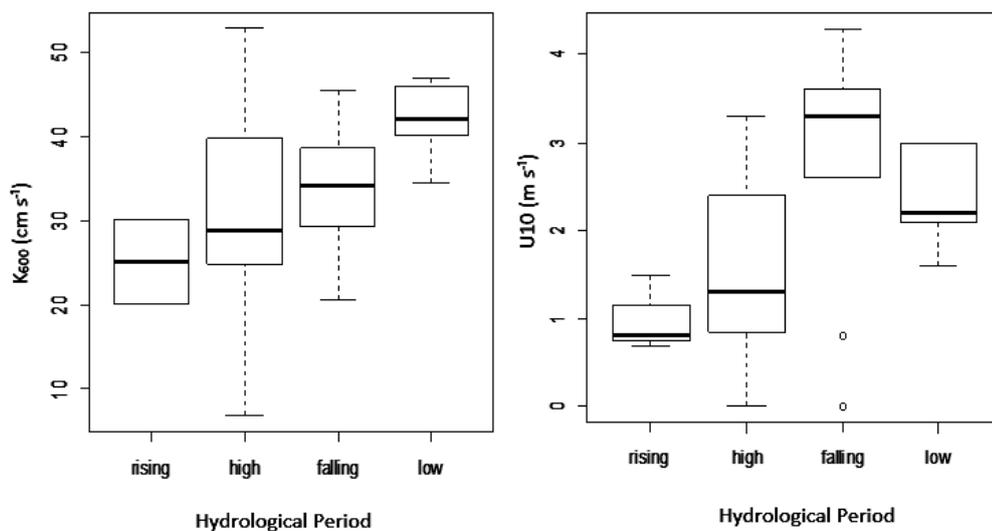
Figure 6: K_{600} and wind speed variability.
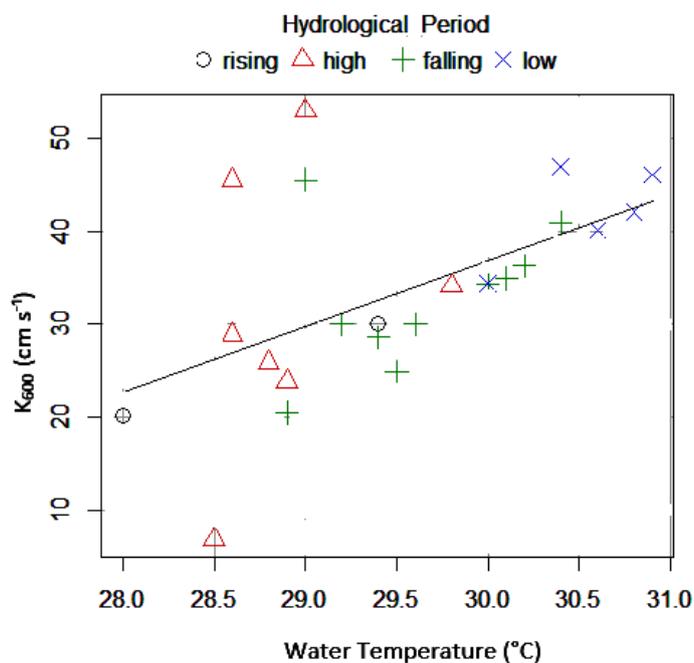
5 **Figure 7: Relation between temperature and K_{600} in the North Channel ($R^2 = 0.46$, $p < 0.05$).**
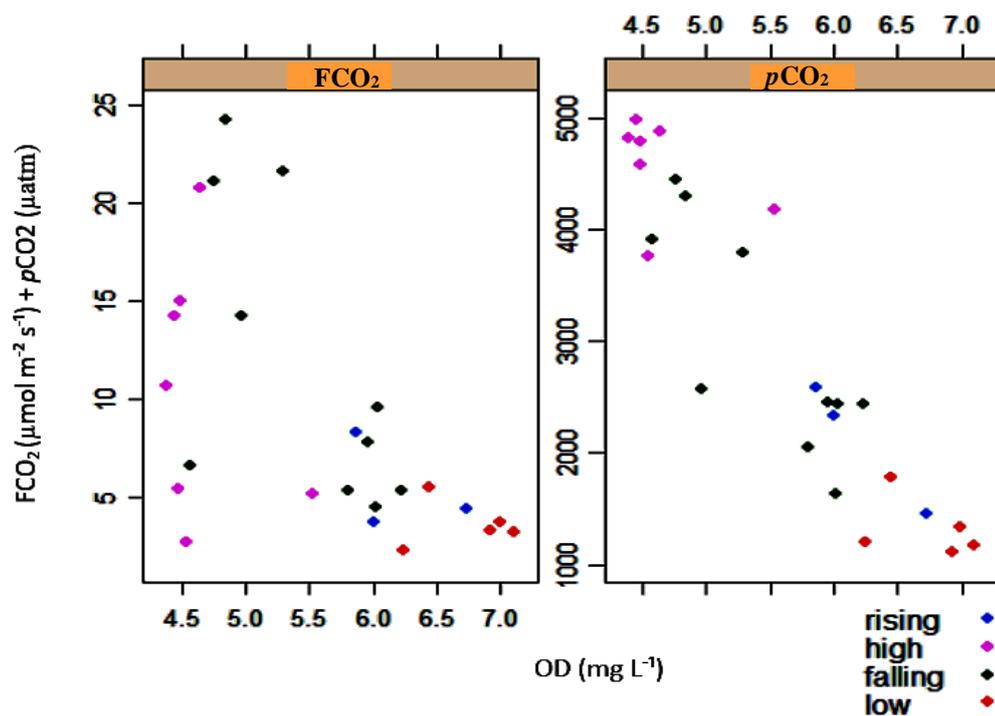
Figure 8: Relation between DO, FCO₂ (R²_FCO2 = 0.33, p < 0.01) and *p*CO₂ (R²_*p*CO2 = 0.85, p < 0.01) in the North Channel.

5

10